Oil & Gas Science and Technology – Rev. IFP, Vol. 54 (1999), No. 6, pp. 703-714

Mechanical Properties of Rocks: Pore Pressure and Scale Effects

M. Boutéca[1] and Y. Guéguen[2]

1 Institut français du pétrole, 1 et 4, avenue de Bois-Préau, 92852 Rueil-Malmaison Cedex - France
2 ENS, Laboratoire de géologie, département TAO, 24, rue Lhomond, 75231 Paris Cedex 5 - France
e-mail: maurice.bouteca@IFP.fr - gueguen@geologie.ens.fr

Résumé — Propriétés mécaniques des roches : pression de pore et effets d'échelle — La pression de pore joue un rôle de première importance dans la considération des propriétés mécaniques des roches. Dans ce domaine, le concept de contrainte effective est essentiel pour aborder les effets mécaniques. Toutefois, son utilisation fréquente a conduit à de nombreuses affirmations trompeuses. Compte tenu des significations diverses accordées à ce concept, nous tentons ici de le clarifier et examinons le domaine d'application de ses divers emplois dans le cadre du comportement mécanique ou des propriétés des roches. À l'échelle macroscopique, la thermodynamique offre un outil puissant pour cerner ce concept. La thermodynamique des processus réversibles ou irréversibles fournit des relations générales d'un intérêt majeur. Mais, compte tenu du fait que les roches sont des systèmes non homogènes, une approche microscopique est nécessaire pour analyser les propriétés mécaniques à partir d'une description des phénomènes à petite échelle. L'approche microscopique est complémentaire de l'approche macroscopique thermodynamique, elle conduit au calcul des propriétés effectives du milieu. Dans ce cadre, la théorie des milieux effectifs est un outil puissant. Les propriétés effectives déduites de l'analyse à l'échelle microscopique peuvent être combinées aux relations issues de la thermodynamique pour interpréter les effets de la pression de pore et les effets d'échelle. Le cas des propriétés élastiques des roches poreuses est plus particulièrement traité à titre d'illustration, compte tenu de l'intérêt qu'il présente et de son importance du point de vue des applications.

Mots-clés : propriétés mécaniques, pression de pore, contrainte effective, effet d'échelle.

Abstract* — *Mechanical Properties of Rocks: Pore Pressure and Scale Effects — *Pore pressure plays a major role when considering rocks mechanical properties. In that field, the concept of effective pressure is a key one to deal with fluids mechanical effects. However, its frequent use has been the source of frequent confusing statements. Because of the various meanings which have been attached to that concept, an attempt is made in this paper to clarify it and examine the validity of its various uses relative to rock mechanical behaviour or rock properties. At a macroscopic scale, thermodynamics provides a powerful tool to investigate this. Reversible or irreversible thermodynamics provide general relationships of great interest. But because real rocks are non homogeneous systems, a microscopic approach is also required in order to analyze the mechanical properties from a description of the small scale processes. The microscopic approach is complementary of the macroscopic thermodynamic one as it leads to the calculation of the effective properties of the medium. In this last approach, effective medium theory is a powerful tool. The effective properties as derived from the microscale can be nicely combined to thermodynamic relations to interpret pore fluid pressure effects and scale effects. The example*

of elastic properties of porous rocks is more specifically emphasized to illustrate this because of both its intrinsic interest and importance as far as applications are concerned.

Keywords: mechanical properties, pore pressure, effective stress, scale effect.

1 MACROSCOPIC SCALE : THE EFFECTIVE STRESS CONCEPT

In the literature, the effective stress concept is applied to three different problems. It is first used for the constitutive equations, it is then extended to rock failure and finally to rock properties. We will review those three categories to clarify the concept.

1.1 The Effective Stress Concept: Constitutive Law

At a macroscopic scale, the effective stress law is defined from an assumption. However, the assumption can be made at two levels. The first level of assumption consists in defining straightforwardly the stress-pressure relationship. Terzaghi's concept is the best known example. However, this stress-strain relationship introduced as an hypothesis must be consistent with the thermodynamic coherence that derives from the strain energy. It can be shown that Terzaghi's law can also be derived from energy considerations.

If the stress-strain relationship is derived from energy, that is from thermodynamics, the consistency of the model is granted. Note that deriving the stress strain relationship from thermodynamics means that the level at which the assumption is made has changed. In other words, the assumption is now made on the strain energy itself.

The macroscopic laws—both in the elastic and plastic domains—correspond to micromechanical mechanisms which are the grain deformation, the cement deformation and the grain displacement.

1.1.1 Terzaghi's Effective Stress - Elastic Domain

Terzaghi's effective stress concept, in this paragraph, is restricted to its application in the elastic domain.

As previously stated, Terzaghi's stress is defined from an assumption on the stresses. It postulates that the pore pressure has no effect on the shear stress and that it decreases the effect of compressive stress by an amount equal to the pore pressure. Thus, the effective stress is defined as:

$$\sigma_{ij}^{eff} = \sigma_{ij} - p\,\delta_{ij} \tag{1}$$

where compressive stresses are taken positive. Expressing the volumetric deformation for an elastic body thus leads to:

$$\varepsilon_v = K_o\,\mathrm{tr}(\sigma^{eff})/3 \tag{2}$$

For an elastic rock, plotting the volumetric deformation as a function of Terzaghi's effective stress, should lead to a straight line.

We performed experiments on a Tavel limestone (Boutéca *et al.,* 1993). Applying an isotropic loading, we increased it in a stepwise manner: the confining pressure is firstly increased, the pore pressure is then increased. The pore pressure increase (Δp_p) is equal to the confining pressure (Δp_c) increase. Hence, at the end of a given step, the effective Terzaghi's stress is equal to its initial value ($\Delta p_c - \Delta p_p = 0$). Such a loading cycle is plotted in Figure 1a and the theoretical stress-strain plot for this limestone is plotted in Figure 1b.

The data as obtained during the experiment are plotted in Figure 1c. The stress-strain line obtained during the confining pressure increase is not the same as the stress-strain line obtained during the pore pressure increase. Applying several cycles as shown in Figure 2a and 2b leads to a behavior that strongly departs from Terzaghi's model. In Figure 2a, we plotted the applied loading cycles. We loaded and unloaded along this stress path. In Figure 2b, we plotted the volumetric strain as a function of Terzaghi's stress. Aside from a very slight hysteresis, the loading and unloading cycles are identical. However in this Terzaghi's plot, the stress strain relationship is not described by a unique straight line. The pore pressure does not exactly play the same role as the confining pressure.

Before moving to another effective stress concept, it is important to notice that although Terzaghi's stress has been defined straightforwardly, its meaning only appears when considering the rock deformation. That is Terzaghi's stress is the one that works in the strain field. Again this leads us towards an identification of the stress based on the energy.

1.1.2 Biot's Effective Stress - Elastic Domain

Starting from a microscale approach, Biot (Biot, 1941) proposed a potential from which he derived the constitutive equation in the elastic domain.

Here, the assumption is no more at the level of the stress but at the level of the thermodynamic potential. The potential is assumed to be quadratic, and, following Coussy (1991), the dual variables are defined as σ, ε, p and m, where m is the fluid mass content in the rock. Deriving the potential, the constitutive law for an isotropic elastic rock is obtained as:

$$\sigma_{ij} - \sigma_{ij}^{o} = \left(K_o - \frac{2G}{3}\right)\mathrm{tr}\varepsilon + 2G\varepsilon_{ij} + b(p - p_o)\delta_{ij} \tag{3}$$

where K_o is the drained bulk modulus of the rock, G, the shear modulus and b, the Biot's coefficient. σ_{ij}^{o} and p_o are initial values.

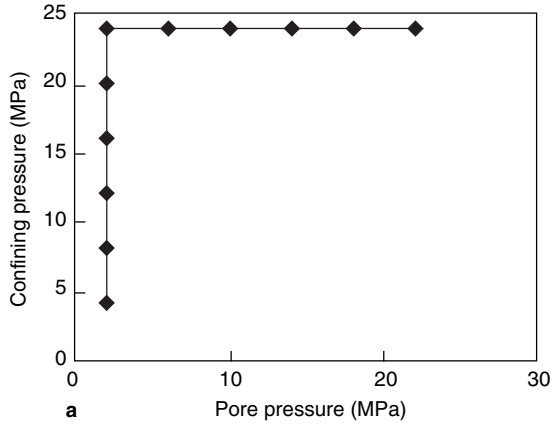

Figure 1a

Isotropic loading cycle ($\Delta p_p = \Delta p_c$).

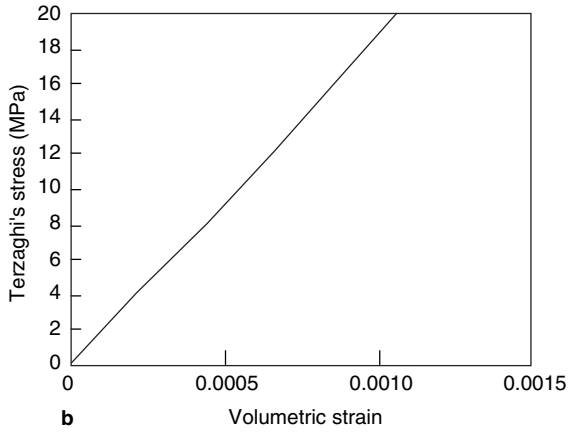

Figure 1b

Theoretical stress-strain plot.

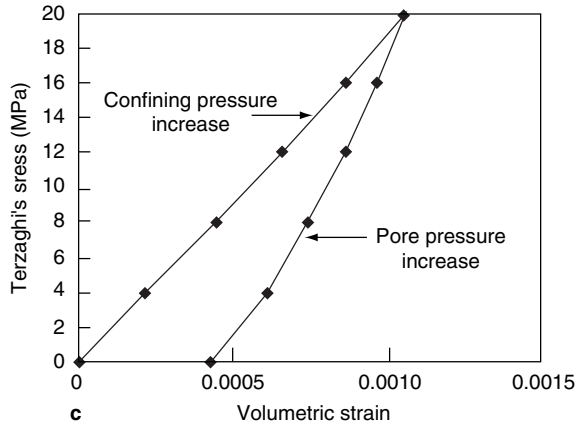

Figure 1c

Experimental results (Tavel limestone).

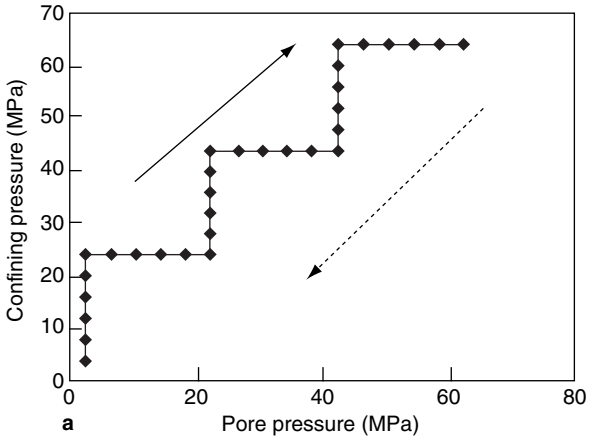

Figure 2a

Loading cycle.

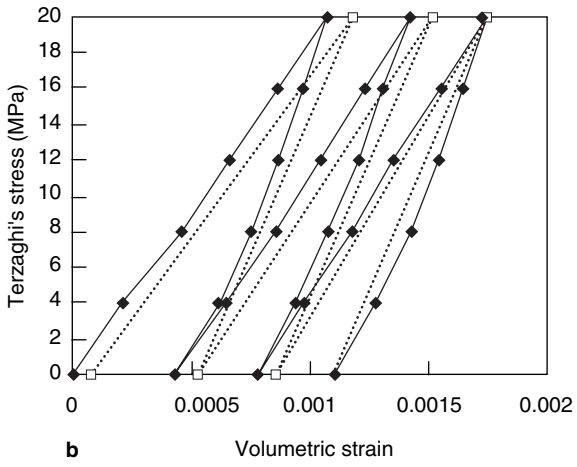

Figure 2b

Experimental results (Tavel limestone).

As a consequence of the constitutive equation, an effective stress can be defined:

$$\sigma_{ij}^{eff} = \sigma_{ij} - b\, p\, \delta_{ij} \tag{4}$$

Formally, Biot's effective stress is very similar to Terzaghi's one, and it can be shown that b varies in the range $[\phi, 1]$, where ϕ is the rock porosity. When b equals 1, one recognizes Terzaghi's stress. More precisely the physical meaning of b can be found from Biot's relation:

$$b = 1 - \frac{K_o}{K_s} \tag{5}$$

where K_s is the skeleton bulk modulus. If the constitutive grains are incompressible ($K_s \to \infty$), then Biot's effective stress and Terzaghi's effective stress are identical.

Note that, from micromechanics considerations, many authors have been deriving an effective stress such that $\sigma_{ij}^{eff} = \sigma_{ij} - \eta\, p\delta_{ij}$. One can find an updated review in Lade and de Boer (1997).

For the experiments shown in Figure 2, we determined the value of the Biot coefficient, it is equal to 0.65. The volumetric strain is plotted as a function of the Biot's stress in Figure 3. The results show a straight line in this plot, in agreement with the theoretical prediction.

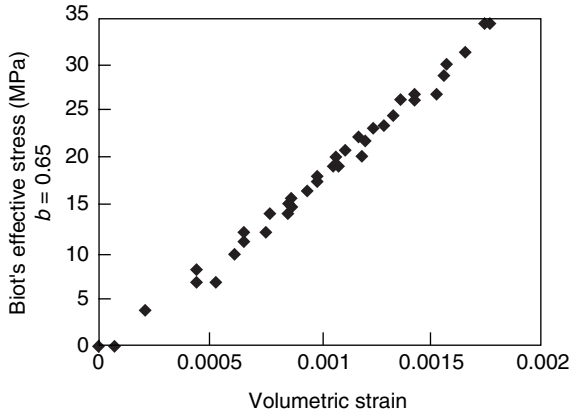

Figure 3

Volumetric strain vs. Biot's stress - Tavel limestone (after Boutéca and Sarda, 1995).

1.1.3 Plastic Domain

The constitutive equations are:

$$\sigma_{ij} - \sigma_{ij}^{o} = \left(K_o - \frac{2G}{3}\right) \mathrm{tr}\varepsilon^{elas} + 2G\varepsilon_{ij}^{elas} + b(p - p_o)\delta_{ij}$$
$$\text{with } \varepsilon = \varepsilon^{elas} + \varepsilon^{plas} \tag{6}$$

where the superscript *elas* stands for the elastic part and the superscript *plas* stands for the plastic part.

It follows from this equation that the stresses inducing the elastic deformation—the ones that insure the mechanical equilibrium—follow the effective stress concept as explained above (see Section 1.1.2). Thus we have:

$$\sigma_{ij}^{'elas} = \sigma_{ij} - b\, p\, \delta_{ij} \quad \sigma' \equiv \sigma^{eff} \tag{7}$$

In the plastic domain, one has to introduce hypotheses on the flow rule to define an effective stress concept. Following Coussy (1991), we assume that the plastic porosity ϕ^p —irreversible change of the pore volume per unit initial volume—is proportional to the volumetric plastic strain, which leads to a new effective stress:

$$\phi^p = \beta_p \varepsilon^p \Rightarrow \sigma'^{plas}_{ij} = \sigma_{ij} - \beta_p p \delta_{ij} \tag{8}$$

If the constitutive grains are incompressible then, one finds back Terzaghi's stress.

1.2 The Effective Stress Concept: Failure Criterion

A failure criterion deals with a limit in a stress space, which implies that the relevant effective stress will be derived from a stress-stress relation and no more from a stress-strain relation.

At the microscopic level, the mechanisms are inter and intragranular cracking leading to rock splitting. It results that the effective stress of the constitutive law and the effective stress at failure do not have to coincide. This is illustrated by our experimental results on the Tavel carbonate (Vincké *et al.*, 1998).

To define the effective stress at failure, we performed three sets of triaxial experiments with three different pore pressures (1 MPa, 10 MPa and 20 MPa). Assuming that the effective stress can be defined as:

$$\sigma_{ij}^{eff} = \sigma_{ij} - \beta\, p\, \delta_{ij} \tag{9}$$

then, by plotting the value at failure in a q (deviatoric stress)-p (total mean stress) plot, one should obtain one failure curve per pore pressure level. Furthermore, $\beta\Delta p_p$ should be the translation vector between a failure curve obtained for a given pore pressure p_p and a failure curve obtained for a pore pressure equal to $p_p + \Delta p_p$ (Fig. 4).

Using this procedure, we determined β for the Tavel limestone and obtained $\beta = 1$. This is shown in Figure 5 where we plotted at failure the deviatoric stress as a function of the mean effective stress ($p - \beta\Delta p_p = p - \Delta p_p$) for the three different pore pressures.

It is interesting to remind the preceeding results for the Tavel limestone:

– constitutive equation: Biot's effective stress

$$\sigma_{ij}^{eff} = \sigma_{ij} - 0.65\, p\delta_{ij};$$

– failure criterion: effective stress $\sigma_{ij}^{eff} = \sigma_{ij} - p\delta_{ij}$.

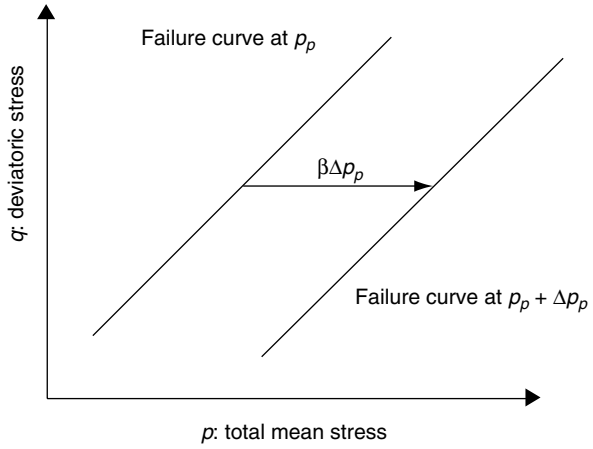

Figure 4

Determination of β-failure criterion.

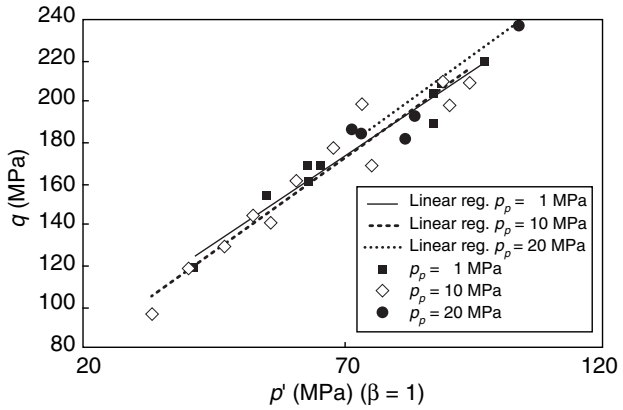

Figure 5

Failure criterion (after Vincké *et al.*)

1.3 The Effective Stress Concept: Rock Properties

The effective stress concept is also applied in the literature to rock properties, both mechanical properties and transport properties. We will first review its meaning in the case of mechanical properties before moving towards transport properties.

1.3.1 Mechanical Properties

To illustrate this, let us consider the experimental data shown in Figure 6 (Boutéca *et al.,* 1994). The drained bulk modulus increases with the confining pressure. Similarly, there is a shift in the curves obtained with a pore pressure equal to 1 MPa and a pore pressure equal to 51 MPa. This kind of result is often interpreted in the literature by defining a relation between the bulk modulus and an effective stress. Thus, nonlinear elasticity—as it is the case here—is treated as incremental linear elasticity with properties depending on an effective stress.

Equation (3) is thus rewritten:

$$\Delta\sigma_{ij}^{eff} = \Delta\sigma_{ij} - b\Delta p\delta_{ij} = \left(\tilde{K}_o - \frac{2G}{3}\right)\mathrm{tr}\Delta\varepsilon + 2G\Delta\varepsilon_{ij} \qquad (10)$$

$$\tilde{K}_o = f(\mathrm{tr}\sigma_{ij} - \kappa p)$$

where the new "effective stress" in f has nothing to do with the one previously introduced for the constitutive law. Instead of relating stresses and strains it relates a coefficient of the constitutive law with stresses and pressure.

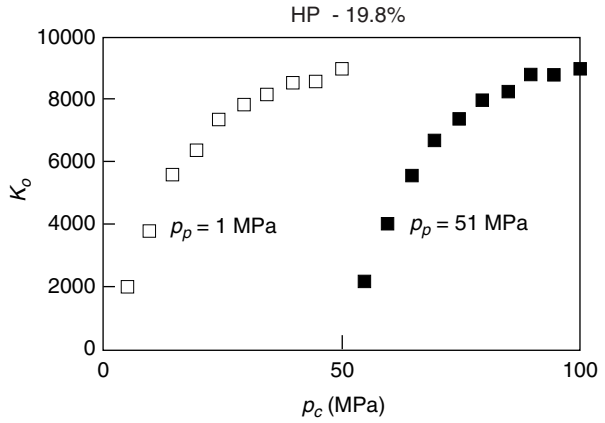

Figure 6

Bulk modulus under drained conditions Reservoir sandstone of initial porosity equal to 19.8% (after Boutéca *et al.,* 1994).

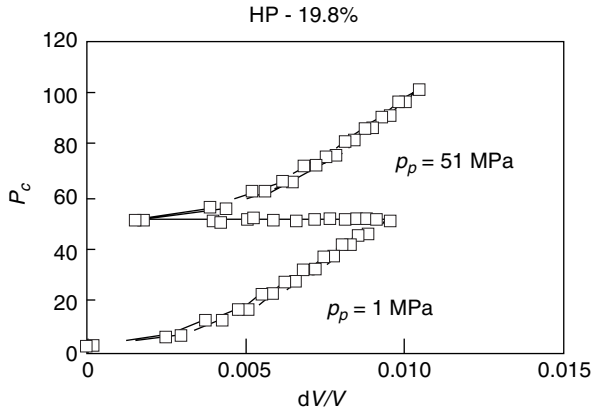

Figure 7

Volumetric strain as a function of the confining pressure (after Boutéca *et al.,* 1994).

At the microscopic scale, the evolution of the rock properties corresponds to Hertz contacts—localization of the stress at the grain contact—and elastic behavior of small cracks in the grain or in the cement. Herein, the model is purely elastic, as opposed to Hertz-Mindlin model where friction is involved at the micro scale (see Section 2.1.3). This departing from the constant value of K_o, is reflected in the stress strain curve which is no longer a straight line and becomes non-linear as shown in Figure 7.

The obvious meaning of Figure 7 is that the hypotheses that led to a linear relationship between stresses and strains as expressed in Equation (3) are no longer valid. Then, one has to come back to the origin of this linear relationship which is the quadratic form of the strain energy. Instead of assuming a quadratic form, let us assume a third order one. Obviously, when deriving with respect to the strain, this will introduce terms of the second order in strain wich will produce non-linearity.

Based on a microscopic description, Biot (1973) defined such a third order potential and we applied it (Boutéca *et al.,* 1994) to the sandstone shown in Figures 6 and 7. It results in a nonlinear tangent drained modulus and a nonlinear tangent Biot coefficient that depend (linearly) on $\varepsilon_v + p/K_s$ where ε_v is the volumetric strain:

$$
\begin{aligned}
d\sigma &= 2G d\varepsilon + 3(\lambda + \lambda^{nl})\, d\varepsilon + 3(b + b^{nl})\, dp_p \\
&= \left[2G + 3(\lambda + \lambda^{nl})\right] d\varepsilon + 3(b + b^{nl})\, dp_p \qquad (11)\\
\lambda^{nl} &= \frac{(4F + 2D)}{3}\left[\varepsilon + \frac{p_p}{K_s}\right] \quad b^{nl} = -\frac{(4F + 2D)}{3K_s}\left[\varepsilon + \frac{p_p}{K_s}\right] \\
\frac{d\sigma}{3} &= K_t d\varepsilon + b_t dp_p \qquad \left(\frac{d\sigma}{3} \equiv p_c\right)
\end{aligned}
$$

where $d\sigma$ is the incremental volumetric stress, F and D are constant rock properties.

The experimental evidence is shown in Figure 8 where we plotted K_t ($\equiv \tilde{K}_o$) as a function of $-(\varepsilon_v + p/K_s)$.

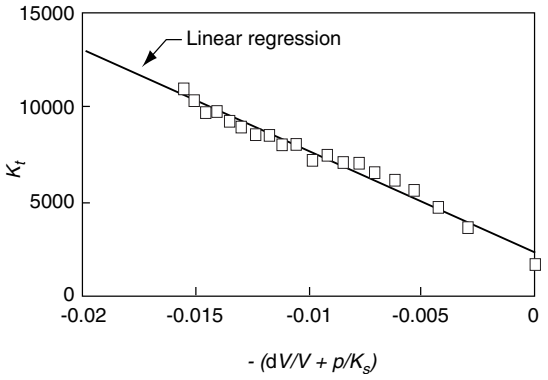

Figure 8

Tangential bulk modulus (after Boutéca *et al.,* 1994).

Hence the nonlinearity is not to be defined through an *a priori* evolution of the bulk modulus, elaborated from experimental curves in some ($K_t = \tilde{k}_o\,(\sigma, p)$) plot. It has to be derived from the enrichment of the thermodynamic potential.

1.3.2 Transport Properties

When measuring transport properties for rocks submitted to pressure and stress evolution (David *et al.,* 1994; Sarda *et al.*, 1998), an effective stress is often defined. In fact it appears that a description at the microscale level is needed.

There is a clear definition of the effective stress for the constitutive law. Hence there is a clear definition of an effective stress for the strains. The next step is to move from strains to permeability which implies a knowledge of the structural evolution at the pore scale. At that scale, cracks and grain deformation or displacement, will play very different roles and their contribution will have to be accounted for in specific ways.

2 MICROSCOPIC SCALE: EFFECTIVE PROPERTIES

Microscopic analysis allows to identify the relevant deformation micromechanisms. It leads to express macroscopic thermodynamic parameters in terms of microvariables which can be obtained from various observations. Such an analysis is a required step in order to discuss possible scale effects on a sound basis. It may be also a crucial point in preventing any extrapolation of a macroscopic law beyond its range of validity. We examine in the following the mechanical behavior and more specifically the elastic properties. This refers to Sections 1.1.2 and 1.3.1 above. We do not consider plastic behavior. The microscopic analysis of failure and that of transport properties is also beyond the scope of this paper. Our restrictive choice is dictated by the fact that elastic wave velocities play a major role for crustal exploration and that our present understanding of elastic behavior and properties is much more advanced than for the other issues considered in Section 1.

2.1 Elastic Moduli of High Porosity Rocks

At a microscopic scale, different descriptions of the rocks are possible, and, depending on the rock nature, some are more appropriate than others. High porosity, poorly consolidated and unconsolidated rocks can be adequately modeled as granular assemblages where contact stiffnesses play the major role. The calculation of elastic constants from micromodels is in that case a two steps procedure: the first step consists in deriving the contact stiffnesses of two grains, and the second one is an averaging process over a random packing of identical spherical particles. As far as elastic properties are concerned, the rock can be viewed as a network of elastic springs, each spring being a grain contact (Fig. 9).

2.1.1 Contact Stiffnesses

All such models rely on the Hertz's and Mindlin's contact theory (Johnson, 1985). In the Hertz model, two identical spherical grains of radius R (Fig. 9) are deformed by a normal force N. The radius of the contact area is:

$$a = \left(\frac{3NR(1-\nu_s)}{8G_s} \right)^{1/3}$$

where ν_s and G_s are respectively the Poisson's ratio and the shear modulus of the grain. The normal displacement of a sphere center relative to the contact area center is $u_n = a^2/R$ and the normal stiffness $D_n = \partial N/\partial u_n$ is:

$$D_n = \frac{4G_s a}{1-\nu_s}$$

Mindlin model considers an additional tangential load T superimposed afterwards on the previous system. Assuming that there is no partial slip in the contact area, the tangential stiffness $D_t = \partial T/\partial u_t$ is:

$$D_t = \frac{8G_s a}{2-\nu_s}$$

where u_t is the tangential displacement of a sphere center relative to the contact area center.

2.1.2 Elastic Moduli

Assuming a random isotropic packing, Digby (1981) derived the effective elastic constants from the contact stiffnesses. He used relationships for stiffnesses which are somewhat different from the above Hertz-Mindlin ones but his averaging procedure constitutes an independent step which allows to express the effective bulk and shear moduli as functions of D_n and D_t, whatever the precise values of the stiffnesses are. With the Hertz-Mindlin stiffnesses, one gets the following expressions for the effective bulk and shear modulus K_{eff} and the G_{eff}:

$$K_{eff} = \frac{C(1-\Phi)}{12\pi R} D_n \qquad G_{eff} = \frac{C(1-\Phi)}{20\pi R} (D_n + 1.5\, D_t)$$

where C is the coordination number (average number of contacts per sphere, which is close to 9 for dense random pack).

2.1.3 Predictions of the Model

A simple test of the above model can be obtained by comparing predicted Poisson's ratio values to measured values on glass beads and high porosity sandstones (Domenico, 1977). As shown by Winkler (1983) the above model predicts values (<0.05) much lower than those observed (0.15) as shown on Figure 10. Although surface roughness may explain some of these discrepancies at low pressures (Palciauskas, 1992; Manificat and Guéguen, 1998), it is likely that other effects have to be accounted for. In the case of sandstones, the presence of cement at grain contacts modify strongly the elastic properties (Dvorkin *et al.,* 1994). Soft cements increase Poisson's ratio so that even a small amount of cement could explain the above discrepancies.

Another test is provided by the pressure dependence. It results from the contact model that the spring constants depend on stress so that the model is a non linear elastic one.

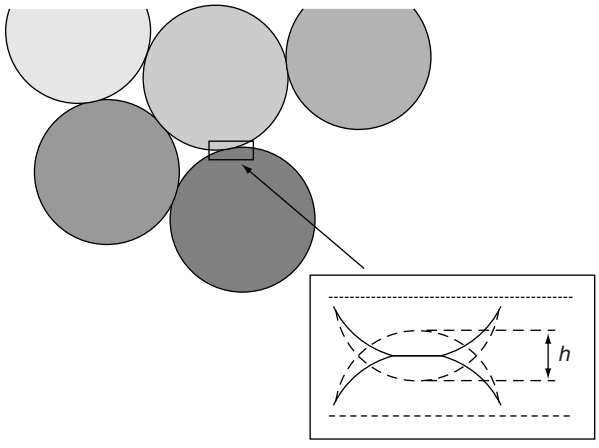

Figure 9

Granular model. The rock is described as a random packing of identical spheres of radius R. Normal displacement at granular contact $h = 2u_n$. Tangential displacement is not shown.

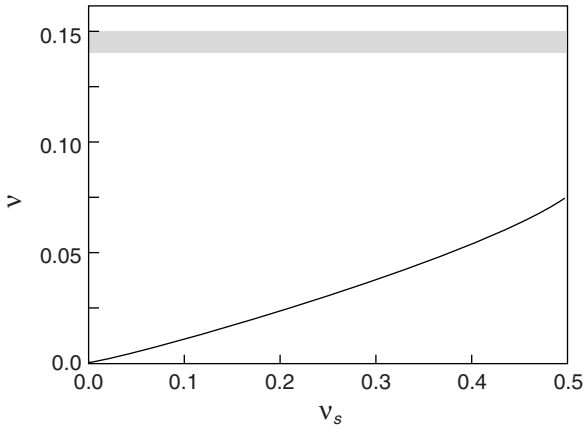

Figure 10

Poisson's ratio of a random packing of spheres (solid line) from Digby's model as compared to high porosity sandstones data (shaded area).

At zero stress, the elastic moduli should vanish and they are predicted to vary as $(P)^{1/3}$ from the above stiffnesses expressions. The results reported by Domenico (1977) for unconsolidated glass beads follow more closely a $(P)^{1/2}$ dependence, whereas those of Toksöz *et al.* (1979) for Berea sandstone show a much weaker dependence. The soft shell model proposed by de Gennes (1996) explains a $(P)^{1/2}$ dependence but is not appropriate for sandstone. Again the presence of cement is likely to affect strongly the pressure dependence. As shown by Wong and Wu (1995), normal stiffness is not sensitive to pressure in a cemented system.

Finally, due to the path dependent nature of contact forces, effective elastic constants are also path dependent. At the microscopic scale, each contact is assumed to be rough. This is why a no slip assumption is made. But this means also that contact forces are not purely elastic since friction is involved. Contact forces are not derivable from a thermodynamic potential. Because of this fundamental complexity of contact models, it is not possible to establish a unique result for elastic constants independently of the stress path trajectory. The medium is not an hyperelastic medium but an hypoelastic one.

2.2 Elastic Moduli of Low Porosity Rocks

The above model breaks down when porosity is below some threshold. Vernik (1997) estimated the threshold value to be approximately 30%. Low porosity rocks can be described by using inclusion-based models that view the rock as a solid matrix with randomly embedded inclusions representing individual pores and cracks (Fig. 11). Several approximate schemes have been used by different researchers in order to achieve this. They have their roots in the effective media theories of physics. This diversity may be confusing and we attempt here to clarify the problem. The calculation of elastic constants from micro-models is obtained through the choice of a specific scheme and of a precise assumption on the geometrical inclusion shape. In the case of pores, the moduli are obtained as functions of porosity Φ or more generally as functions of the ratio Φ/α for ellipsoidal pores of aspect ratio α (Guéguen and Palciauskas, 1994). In the case of cracks (which can be considered as the limiting case of zero volume inclusions), the moduli are functions of the crack density parameter defined in 2-*D* as $\rho = 1/A \sum (l_i)^2$ where each rectilinear crack has a length l_i and A is the area of the considered element.

2.2.1 Effective Media Schemes

The elastic moduli are calculated by replacing the heterogeneous rock by a simple homogeneous equivalent medium. The properties of this equivalent medium are the effective properties. The use of the word effective here should not be confused with that of Section 1 where effective stress has been discussed. The effective stress concept assumes that the medium is statistically homogeneous and replaces the real rock by an equivalent homogenized medium. The purpose of Section 2 is precisely to examine how the elastic properties of this equivalent (effective) medium are derived.

The simplest model is the one which assumes negligible interactions between inclusions. It may be called a first order perturbation scheme. In that case, the medium is a simple

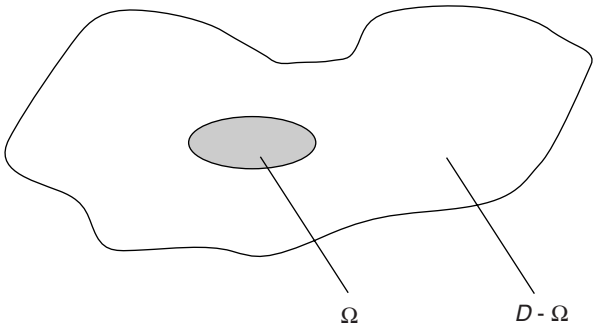

Figure 11

Inclusion model: a pore or crack is described as an inclusion of specific shape (Ω) included in the rock matrix ($D - \Omega$).

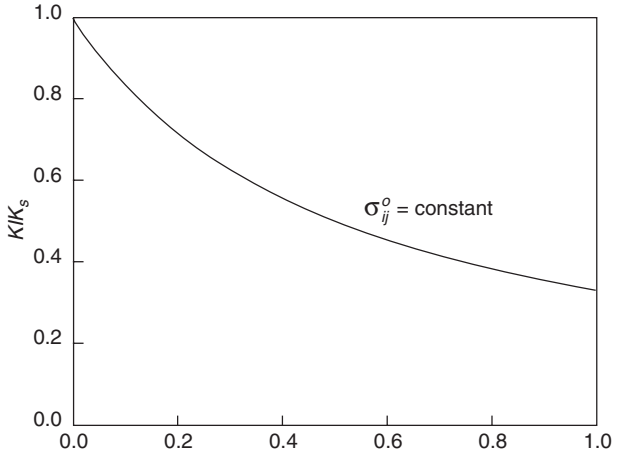

Figure 12

Normalized bulk modulus as a function of porosity for the inclusion model. The assumptions are: non interacting inclusions and spherical pores. The matrix bulk modulus is K_s = 38 GPa, the matrix shear modulus is G_s = 22.8 GPa. The pores are saturated with a fluid of bulk modulus K_f = 2.2 Gpa.

composite which behaves as if it was made of a single inclusion within a matrix. The elastic compliances are derived by submitting this medium to a constant stress at infinity, and the compliances are found to be linear functions of porosity Φ or crack density ρ. Elastic stiffnesses are thus non linear functions of Φ or ρ (Fig. 12). In the limit of a diluted concentration of inclusions, linearization of these expressions is however possible (Le Ravalec and Guéguen, 1996a).

More sophisticated models account for inclusions interactions in some approximate ways. Following Kachanov (1993), we can consider that most of these schemes calculate the effective elastic constants by analyzing one isolated inclusion in either an effective matrix or an effective field. This corresponds to a basic subdivision of effective media schemes in two groups:

– The effective matrix scheme assumes that the inclusion is placed within a matrix which has effective moduli. If the inclusions are placed in a single step, this scheme is known as the self-consistent one. The interactions between inclusions are approximately taken into account by replacing the background medium with the as-yet-unknown effective medium. The self-consistent scheme is an implicit scheme which assumes the solution known in order to calculate it. If the inclusions are placed in infinitesimal increments, the scheme is an iterative one and is known as the differential self-consistent scheme (Le Ravalec and Guéguen, 1996a).
– The method of effective field approximates inclusions interactions by assuming that an inclusion is submitted to an effective stress field. This field is not the one applied to the medium but some average of the real stress field which takes approximately into account the inclusions interactions. The simplest effective field is the volumetric average (Mori-Tanaka method).

2.2.2 Predictions of the Model

Effective medium theory has been successfully used to predict the properties of many heterogeneous systems. The various possible schemes have each some specific advantages and drawbacks which are discussed below.

The self-consistent (effective matrix) scheme predicts a strong decrease of moduli down to zero at some cut-off porosity value, or crack density value (Fig. 13). For that reason, this model has been attractive and widely used. It can be shown however that this cut-off does not have a physical meaning and that it corresponds to an extrapolation of the model beyond its range of validity as explained below (Kachanov, 1993, Guéguen *et al.,* 1997). The self-consistent model overestimates the moduli decrease.

The differential self-consistent (effective matrix) scheme does not predict any cut-off and exhibits a less severe decrease of moduli with pores/cracks content. It predicts remarkably well the porosity dependence, at least for spherical inclusions (Fig. 13a). Since the pores and cracks are added incrementally, this model can be extended to consider various families of pores and cracks, introducing for instance a range of aspect ratios. But the elastic moduli depend on the order in which the incremental additions are done. This is a drawback specific to that method. A possible way to go around this difficulty is to realize several numerical simulations with the same input data but with a different

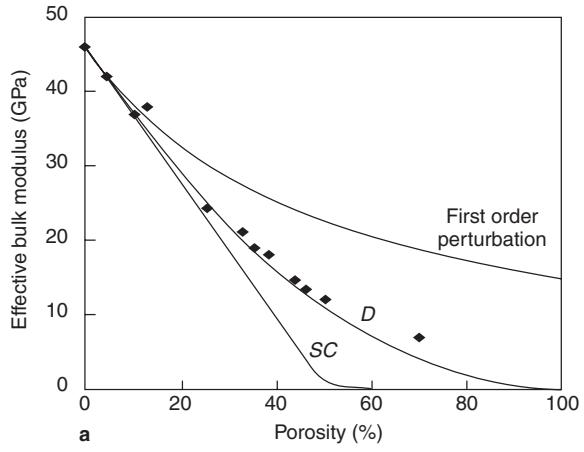

Figure 13a

Effective Bulk moduli for glass foam samples as a function of porosity (Walsh *et al.,* 1965). The predictions are those of the first order perturbation model (noninteracting cracks), the self-consistent model and the differential self-consistent model.

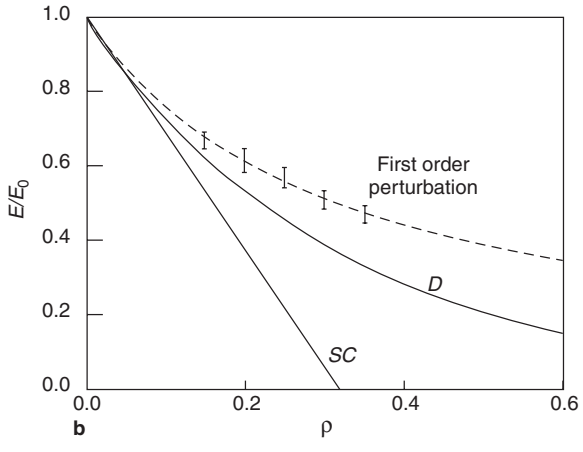

Figure 13b

Effective Young moduli for randomly oriented cracks as a function of crack density. Numerical simulations are shown as vertical bars (Kachanov, 1993). The predictions are the same as above.

order of introduction of inclusions. Averaging over a large number of numerical simulations provides then valid results. In practice, it has been shown that one hundred simulations is sufficient to get stable solutions (Le Ravalec and Guéguen, 1996a).

The effective field method appears to be a better approximation in general than the effective matrix method. An important and interesting result (Kachanov, 1993) is that, in the case of randomly oriented cracks, the effective moduli predicted with the Mori-Tanaka method are identical to those obtained from the approximation of noninteracting cracks (i.e., from first order perturbation calculations). Kachanov pointed out clearly that this is not a coincidence but results from the fact that introducing zero volume cracks does not change the average stress in a solid if tractions are prescribed on the boundary. Consequently, the average effective field in the Mori-Tanaka approximation is exactly the original field and thus the calculation is that of a noninteracting approximation. Numerical simulations show that the non-interacting cracks approximation is the best one in that case. (Kachanov, 1993). If cracks are described as flat ellipsoids of nonzero volume, the differential self consistent results and the noninteracting results remain very close (Le Ravalec and Guéguen, 1996b).

Up to what degree of heterogeneity can effective media theory be used? This theory is an approximation which relies on the assumption that the medium is statistically homogeneous. As stated above, the critical thresholds or cut-off derived from the self consistent scheme do not fit with real data. This is not surprising since the existence of such thresholds is linked to clustering effects which become important in a strongly nonhomogeneous medium (Guéguen *et al.,* 1997). Using the previous scheme near the threshold is clearly extrapolating it beyond its range of validity. The differential scheme should be preferred as it does not exhibit such thresholds and accordingly does not overestimate so much the decrease of moduli. The differential scheme itself has also a limited range of validity however. In the case of a strongly heterogeneous medium, percolation theory is the appropriate tool since clustering effects are a central issue of percolation theory. It can be shown (Guéguen *et al.,* 1997) that various thresholds have to be distinguished depending on the properties of interest. In particular, the mechanical threshold and the permeability threshold are completely different. For cracked rocks, the first one is reached at high crack density (of the order of 1) but the second one is reached at much lower values (of the order of 0.1).

2.3 Pore Pressure and Scale Effects: Combining Micro- and Macroanalysis

We focus in the following on the elastic properties because of their importance for underground exploration and also because they provide a nice example in which combining micro- and macroanalysis proves to be very fruitful.

2.3.1 Poroelasticity

Poroelasticity describes the mechanical behaviour of a saturated porous rock at moderate pressure and temperature conditions (Biot, 1941; Rice and Cleary, 1976). As discussed in Section 1.1.2, it is a thermodynamic theory which expresses strains as linear functions of effective stresses. It can be extended to nonlinear behaviour (Biot, 1973; Boutéca *et al.,* 1996) and to anisotropic media (Brown and Korringa, 1975) but we restrict here to the simple case of linearity and isotropy. A basic result of this theory is that the drained bulk modulus K_d is related to the undrained bulk modulus K_u through the following equation (Gassmann equation):

$$K_u = K_d + \frac{b^2}{\dfrac{\Phi}{K_f} + \dfrac{(b-\Phi)}{K_s}}$$

Both shear moduli, drained and undrained, are identical. The b coefficient has been defined in Section 1.1.2.

Poroelasticity does not provide of course any information on the above moduli. But the micromodels described in Section 2 do. Both drained and undrained moduli are effective moduli. The drained modulus corresponds to the situation where fluid can flow at constant pressure. It can be obtained from effective media theory by considering dry inclusions, i.e. empty cracks and pores (low porosity rocks) or a dry granular assemblage (high porosity rocks). If the drained modulus is known, using the above equation provides then the undrained modulus. It is this last one which has to be used for elastic waves velocities.

2.3.2 Scale and Frequency Effects

Pushing the analysis one step further, it is possible to examine scale and frequency effects. The fluctuating stresses caused by the passing of a seismic wave in a porous saturated rock induce pore pressure gradients on the scale of individual pores and cracks. At high frequencies, the gradients are unrelaxed and the rock is stiffer than at low frequencies where pore pressures are equilibrated through the pore space. Gassmann equation applies at low frequencies (<100Hz) because in that case there is sufficient time for fluid to flow so that fluid pressure is equilibrated. Laboratory ultrasonic measurements (10^6 Hz) are likely to be high frequency measurements in the above sense of an unrelaxed pore fluid state. How can we calculate the appropriate elastic moduli in such a situation? The answer is given by using effective media models once more, but with fluid inclusions and no longer with dry inclusions. For instance the differential self-consistent scheme considers that the inclusions are isolated. The pore fluid pressure within each inclusion is consequently variable from one to the other. This is an unrelaxed state and

the modulus derived from this model is an unrelaxed one. Combining porelasticity and effective media theory allows thus to derive high and low frequency moduli and to predict elastic wave dispersion (Fig. 14) (Le Ravalec *et al.,* 1996a and 1996b).

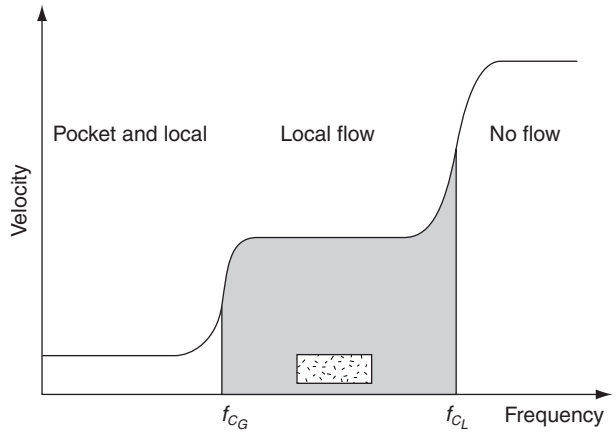

Figure 14

Velocity dispersion resulting from local and pocket flow. Low frequency velocity is derived from Gassmann equation and effective media theory. High frequency velocity is derived from effective media theory.

A realistic situation is that of partial saturation. We have so far only considered dry or totally saturated rocks. The saturation may be variable from one point to the other. In that case, one can describe the rock as made of pockets (or patches) of saturation S_1 in a matrix of saturation S_2. Both the pockets and the matrix are made of a mixture of dry and saturated inclusions. Using for instance the differential self-consistent scheme of effective media theory, it is possible to derive the unrelaxed and relaxed moduli of a pocket and of the matrix. If the frequency is low enough for the fluid pressure to be equilibrated at the pocket scale, but high enough to be unequilibrated at the matrix scale, fluid pressure gradients exist at the pocket scale and velocity dispersion is again expected (Fig. 14).

The dispersion mechanisms at local scale and at pocket scale are frequency and scale effects which have to be taken into account in many different situations: extrapolation from laboratory data to field data, interpretation of saturation hysteresis, interpretation of seismic waves anomalies.

CONCLUSION

The concept of effective stress in rock mechanics covers very different notions, as summarized in Figure 15. It firstly applies to the relationship between stresses and strains. There, the effective stress concept, as pointed out by Coussy (1991) is a consequence of the constitutive law. At the microscopic level, the corresponding mechanisms to be considered are the grain deformation, the cement deformation and the grain displacement.

The concept is then applied to criteria (shear failure, limit of the elastic domain, plasticity criterion) and the effective stress concept involves a stress-stress relation. At the microscopic level, the mechanisms are inter and intra-granular cracking leading to rock splitting.

The concept is then applied to rock properties changes. For mechanical properties the relation between mechanical properties, stresses and pressure should be derived from energy considerations. For transport properties, it should be derived from microscopic considerations, linking structural changes with pressure and macroscopic stresses.

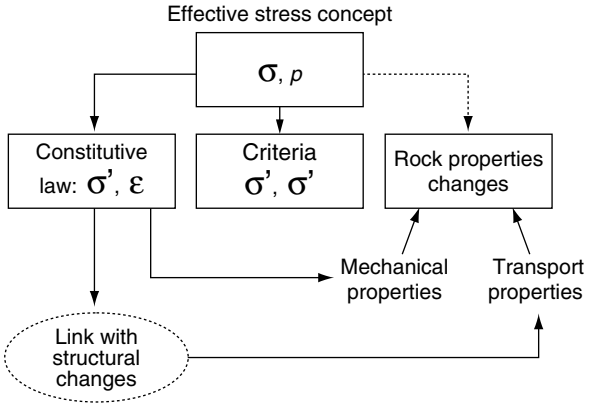

Figure 15

The effective stress concept in saturated media.

At a microscopic scale, use of specific descriptions of the rock microstructure allows to calculate the effective properties of the rock. Such a microscopic description is complementary of the macroscopic one. Combining both allows to investigate scale effects. The example of elastic properties has been developed and it has been shown that the frequency dependence of elastic waves in saturated rocks is in fact a scale effect which can be accounted for within the framework of poroelasticity and effective medium theory

ACKNOWLEDGMENTS

The authors would like to thank their colleagues Jean-Paul Sarda, Pascal Longuemare, Olivier Vincké and Atef Onaisi for fruitful discussions. Olivier Coussy and Luc Dormieux have contributed to the process of clarifying the ideas herein presented. We also benefited from discussions with Pr. Teng-Fong Wong and Pr. Jim Rice.

REFERENCES

Biot, M.A. (1941) General Theory of Three Dimensional Consolidation. *J. Appl. Phys.,* **12**, 155-164.

Biot, M.A. (1973) Nonlinear and Semilinear Rheology of Porous Solids. *J. Geoph. Res.,* **78**, 23, 4924-4937.

Boutéca, M.J., Bary, D. and Maury, V. (1993) An Experimental Study of the Contribution of the Pore Volume Change to Production Within the Framework of Biot's Theory. *Proceedings of the 1993 Society of Core Analysts Technical Conference.*

Boutéca, M.J., Bary, D., Piau, J.M., Kessler, N., Boisson, M. and Fourmaintraux D. (1994) Contribution of Poroelasticity to Reservoir Engineering: Lab Experiments, Application to Core Decompression and Implication in HP-HT Reservoirs Depletion. *Paper SPE/ISRM* 28093.

Boutéca, M.J. and Sarda, J.P. (1995) Experimental Measurements of Thermoporoelastic Coefficients. *Mechanics in Porous Media,* Charlez, P. (ed.), Balkema, 31-41.

Brown, R. and Korringa, J. (1975) On the Dependence of the Elastic Properties of a Porous Rock on the Compressibility of the Pore Fluid. *Geophysics,* **40**, 608-616.

Coussy, O. (1991) *Mécanique des milieux poreux,* Éditions Technip, Paris.

David, C., Wong, T.F., Zhu, W. and Zhang, J. (1994) Laboratory Measurement of Compaction - Induced Permeability Change in Porous Rocks: Implications for the Generation and Maintenance of Pore Pressure Excess in the Crust. *PAGEOPH,* **143**, 1/2/3.

De Gennes, P.G. (1996) Static Compression of a Granular Medium: the Soft Shell Model. *Europhysics Letters,* **35**, 145-149.

Digby, P.J. (1981) The Effective Elastic Moduli of Porous Granular Rocks. *J. Appl.Mech.,* **48**, 803-808.

Domenico, S.N. (1977) Elastic Properties of Unconsolidated Porous Sand Reservoirs. *Geophysics,* **42**, 1339-1368.

Dvorkin, J., Nur, A. and Yin, H. (1994) Effective Properties of Cemented Granular Materials. *Mech. Mater.,* **18**, 351-366.

Guéguen, Y., Chelidze, T. and Le Ravalec, M. (1997) Microstructures, Percolation Thresholds, and Rock Physical Properties. *Tectonophysics,* **279**, 23-35.

Guéguen, Y. and Palciauskas, V. (1994) *Introduction to the Physics of Rocks,* Princeton University Press, Princeton, NJ.

Johnson, K.L. (1985) *Contact Mechanics,* Cambridge University Press.

Kachanov, M. (1993) Elastic Solids with Many Cracks and Related Problems. *Adv. Appl. Mech.,* **30**, 259-445.

Lade, P.V. and de Boer, R. (1997) The Concept of Effective Stress for Soil, Concrete and Rock. *Géotechnique,* **47**, 1, 61-78.

Le Ravalec, M., and Guéguen, Y. (1996a) High and Low Frequency Elastic Moduli for a Saturated Porous/Cracked Rock-Differential Self-Consistent and Poroelastic Theories. *Geophysics,* **61**, 1080-1094.

Le Ravalec, M. and Guéguen, Y. (1996b) Comment on "The Elastic Modulus of Media Containing Strongly Interacting Antiplane Cracks" by Paul M. Davis and Leon Knopoff. *Geophys. Res. Lett.,* **101**, 25373-25375.

Le Ravalec, M., Guéguen, Y. and Chelidze, T. (1996a) Elastic Waves Velocities in Partially Saturated Rocks: Saturation Hysteresis. *J. Geophys. Res.,* **101**, 837-844.

Le Ravalec, M., Guéguen, Y. and Chelidze, T. (1996b) The Magnitude of Velocity Anomalies Prior to Earthquakes. *J. Geophys. Res.*, **11**, 217-223.

Manificat, G., and Guéguen, Y. (1998) What Does Control Vp/Vs in Granular Rocks? *Geophys. Res. Lett.,* **25**, 381-384.

Palciauskas, V. (1992) Compressional to Shear Wave Ratio of Granular Rocks: Role of Rough Grain Contacts. *Geophys. Res. Lett.,* **19**, 1683-1686.

Rice, J.R., and Cleary, M. (1976) Some Basic Stress Diffusion Solutions for Fluid Saturated Porous Media with Compressible Constituents. *Rev. Geophys. Space Phys.,* **14**, 227-241.

Sarda J.P., Ferfera, F.M.R., Vincké, O., Boutéca, M. and Longuemare, P. (1998) Experimental Study of the Stress Paths Influence on Monophasic Permeability Evolution. *SCA* 9827.

Toksoz, M.N., Johnston, D.H. and Timur, A. (1979) Attenuation of Seismic Waves in Dry Saturated Rocks: I Laboratory Measurements. *Geophysics,* **44**, 681-690.

Vernick, L. (1997) Predicting Porosity from Acoustic Velocities in Siliciclastics: A New Look. *Geophysics,* **62**, 1, 118-128.

Vincké, O., Boutéca, M.J., Piau, J.M. and Fourmaintraux, D. (1998) Study of the Effective Stress at Failure. *Proceedings of the Biot Conference on Poromechanics.*

Walsh, J.B., Brace, W.F. and England, A.W. (1965) Effect of Porosity on Compressibility of Glass. *J. Am. Ceram. Soc.,* **48**, 605-608.

Winkler, K.W. (1983) Contact Stiffness in Granular Porous Materials: Comparison between Theory and Experiment. *Geophys. Res. Lett.,* **10**, 1073-1076.

Wong, T.F., and Wu, L.C. (1995) Tensile Stress Concentration and Compressive Failure in Cemented Granular Material. *Geophys. Res. Lett.,* **22**, 1649-1652.

Final manuscript received in July 1999